Earth's response to surface mass loads: inferences from ocean tide loading

Peter Clarke[1], Machiel Bos[2], Nigel Penna[1]
[1] School of Civil Engineering and Geosciences, Newcastle University, UK
[2] Institute D. Luis, Universidade Beira Interior, Covilhã, Portugal

Peter.Clarke@newcastle.ac.uk

1. Introduction

Earth is an imperfectly elastic body whose various layers can each be characterised by a quality factor *Q* related to the fractional energy loss per deformation cycle. One effect of this anelasticity is that the response to forcing is attenuated and delayed (dissipation), the latter being equivalent to a complex-valued shear modulus μ. *Q* is measured at seismic periods (~1 s to ~1 h) and appears to be constant across these timescales. It is lowest for the asthenospheric upper mantle where $Q \sim 80$ at seismic periods in contrast to $Q > 300$ in the majority of the mantle.

According to absorption band theory [1-4], *Q* will decrease at longer periods, then increase once the unknown upper limit of the absorption band is reached, before decreasing again once steady-state viscous behaviour dominates. Knowing the timescales of these transitions is critical for accurate modelling of ocean tide and seasonal loading.

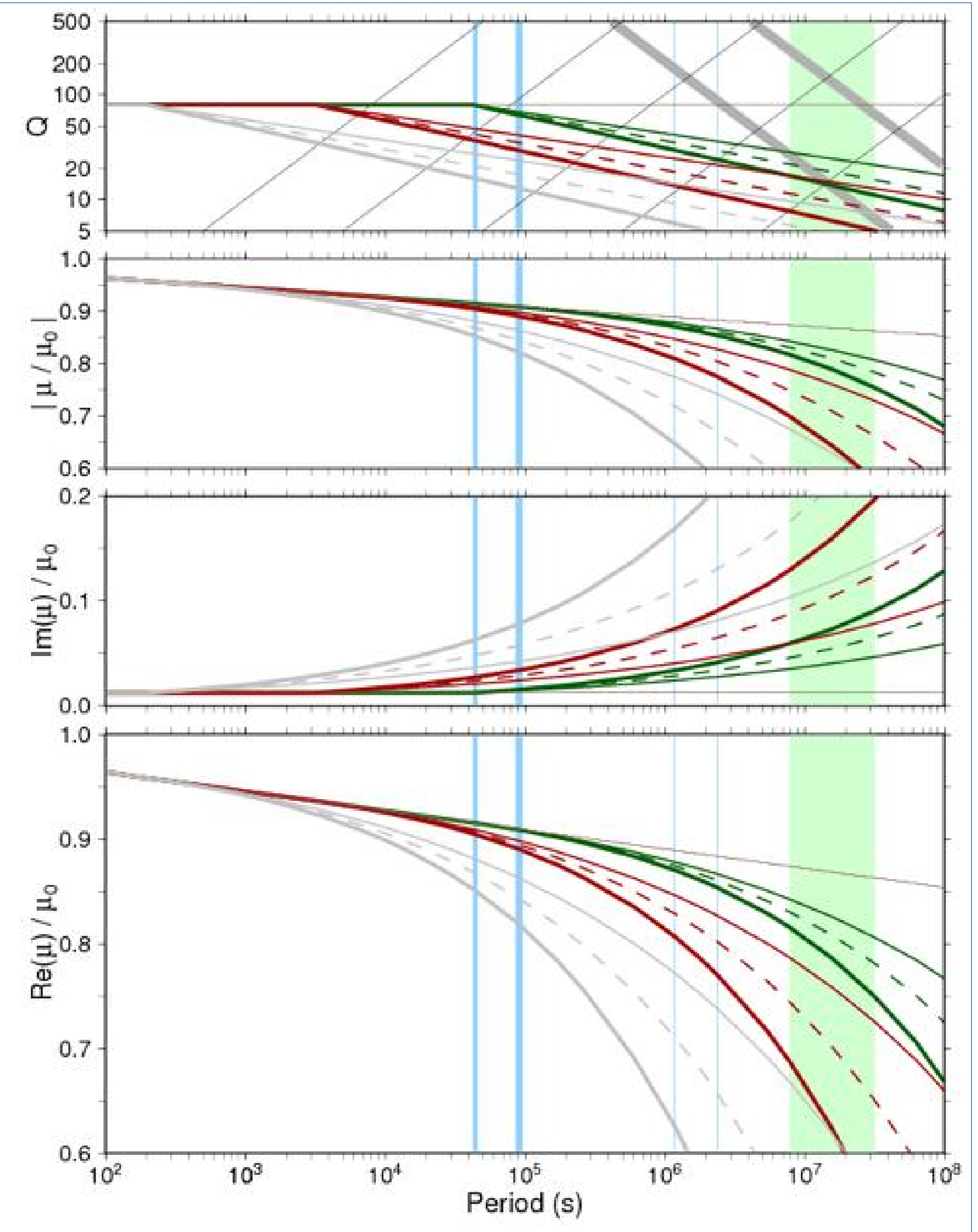

Figure 1. Upper panel: Variation of asthenospheric *Q* with period *T*, for the PREM Earth model [5] with absorption band frequency dependence above *T*=200 s (pale grey), *T*=54 m (red), and *T*=12 h (green). *Q* then decays as $T^{-\alpha}$ (α=0.2, 0.25, 0.3 shown as thin, dashed and bold lines; constant *Q* shown as very thin line) until the upper period of the absorption band is met (thin black lines ascending to the right for *Q* proportional to *T*). At longer timescales, steady-state rheology with *Q* proportional to 1/*T* dominates, shown for Maxwell rheology with viscosities 10^{18} and 10^{19} Pa s (thick grey lines).
Lower panels: Variations of the real and imaginary parts of μ, and its magnitude (normalised by the elastic value μ_0), for the $Q = T^{-\alpha}$ models described above.
Vertical bands show semi-diurnal, diurnal, fortnightly and monthly tidal periods (blue), and seasonal periods (green).

2. Evidence from ocean tide loading

Using GPS observations in western Europe, we have shown previously [5-6] that Earth's response to semi-diurnal ocean tide loading (OTL) requires that asthenospheric anelasticity be taken into account. This is not the case in Green's functions commonly used to compute OTL by the geodetic community. Our observations show that *Q* is independent of *T* (or only very weakly dependent) at least as far as the semi-diurnal tidal band, in contrast to earlier geodynamic predictions [e.g. 3] which were based on a lower *Q* at seismic periods. This suggests that anelastic effects could be relevant even to seasonal timescales, at which point viscous rheology dominates.

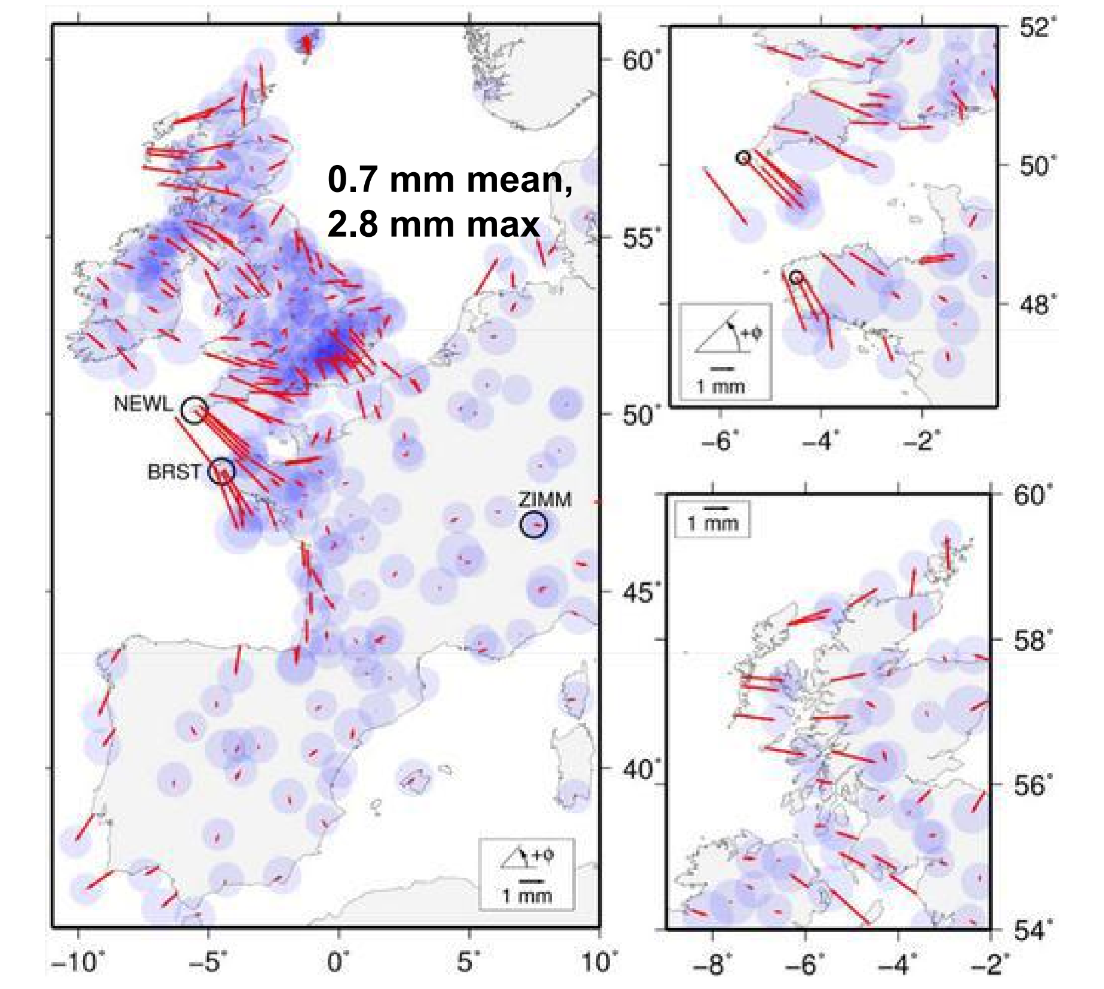

Figure 2a. Residual phasors of M2 harmonic vertical. displacements at 259 GNSS sites, compared with computed OTL using the FES2012 ocean tide model and a purely elastic Earth model based on PREM (from [6]).

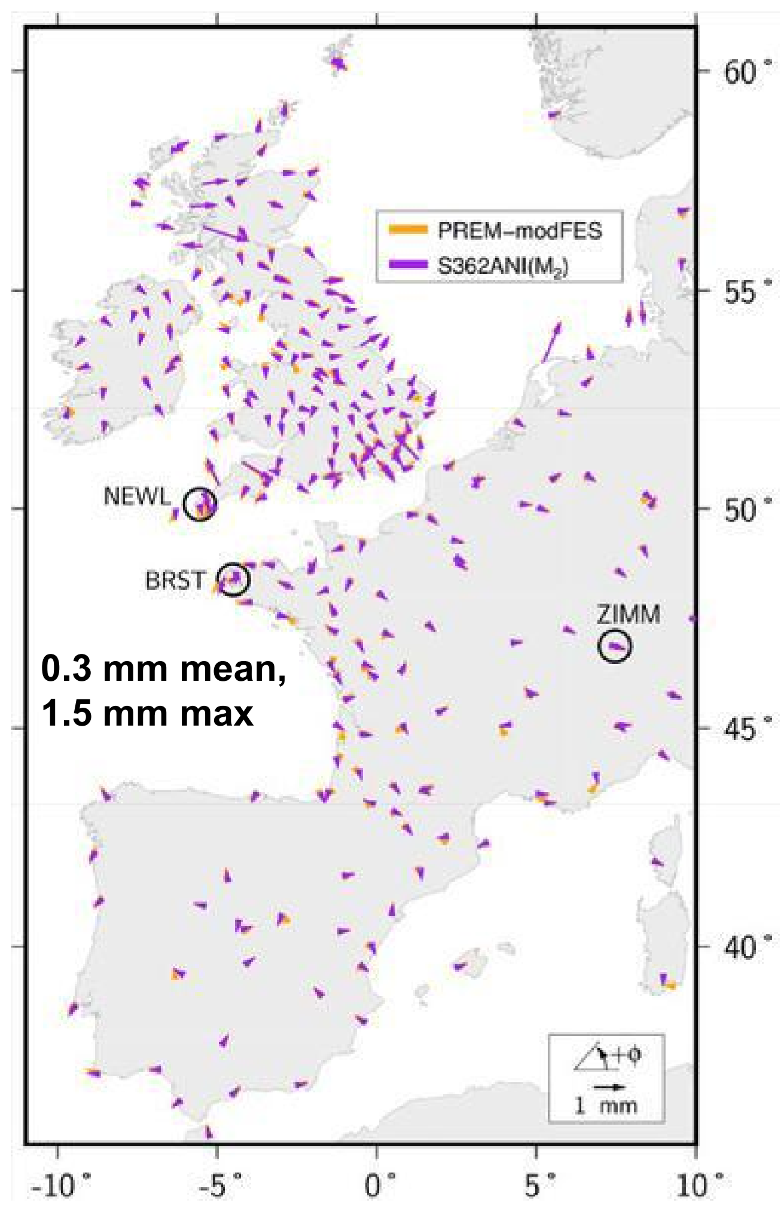

Figure 2b. Residual M2 vertical harmonic phasors using an empirically-tuned variant of PREM including asthenospheric anelasticity [6], and using the S362ANI [7] anelastic Earth model.

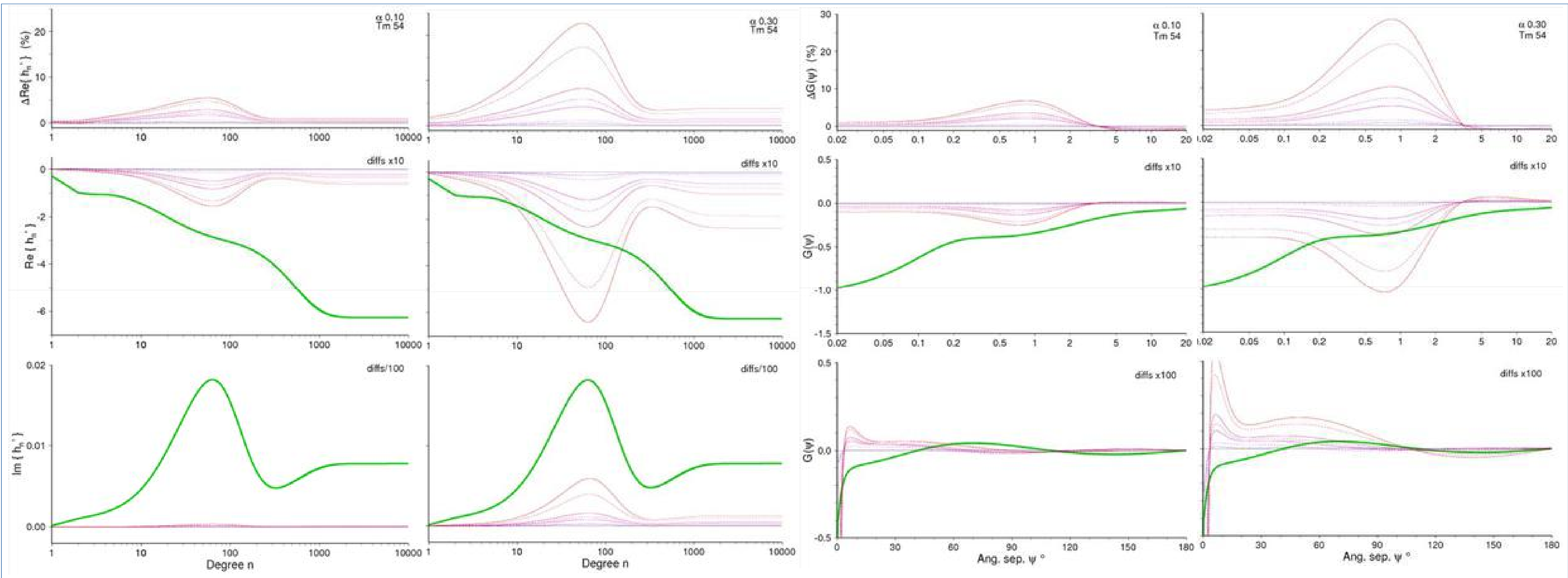

Figure 3. Real and imaginary vertical load Love numbers (L) and the real-valued part of the vertical loading Green's function (R) for an anelastic PREM-based model with α=0 at near-seismic (3 h) period, and differences from these at semi-diurnal, weekly, diurnal, fortnightly, monthly, semi-annual and annual periods (thin lines coloured blue through red, scaled). Plots are shown for weak (α=0.1) and strong (α=0.3) frequency dependence of *Q*.

3. Implications for Earth models

Anelastic behaviour in the asthenosphere will result in increasing changes in the response to surface mass loads at longer periods, particularly if *Q* becomes frequency-dependent. These changes will be most prominent in the Love numbers for spherical harmonic degrees 10-100, equivalent to load distances of up to ~300 km in the Green's functions. These spatial scales correspond to significant mass loads acting on the Earth's surface: not only ocean tide loading but seasonal atmospheric pressure and hydrological loading. Measurement and modelling of the latter in particular depends on knowing accurate values of the Love numbers *h'* (for GNSS and other geometric techniques) and *k'* (for GRACE).

4. Consequences for seasonal loading

We illustrate the effect of Earth model on seasonal surface mass loading by considering the difference between vertical displacements computed using Love numbers appropriate to short periods (3 h) and those for annual periods for a range of dependencies of *Q*. These differences can amount to 5% of the signal, even for weak frequency dependence of *Q*, and exceed 10% (> 1 mm) for larger α, which corresponds to a *Q* value similar to that of a weak viscous rheology at annual periods.

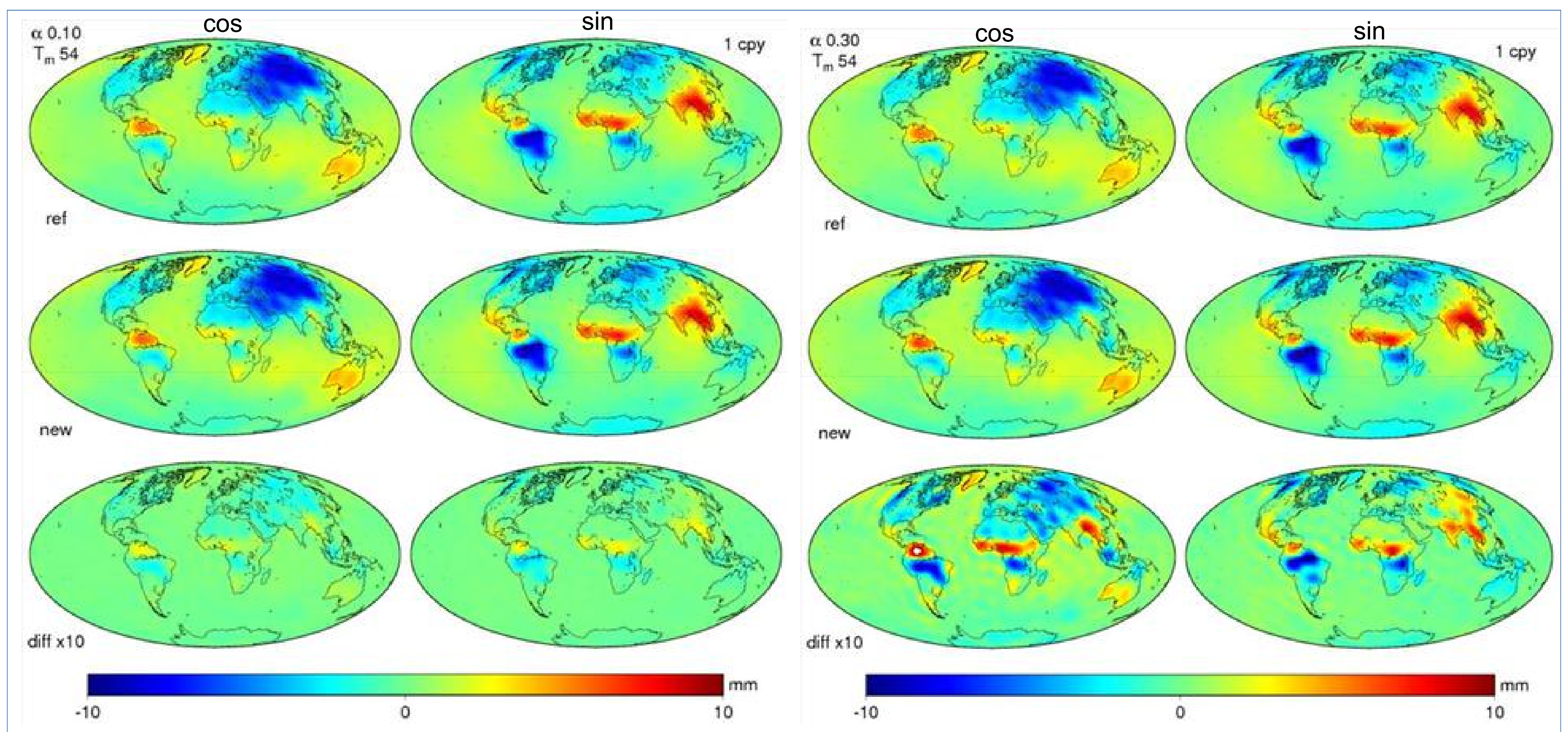

Figure 4. Illustrative annual cosine and sine surface mass loading displacement, using a fit to the CPC/NCEP hydrology and atmospheric pressure models, computed using short-period Love numbers (top) and those for an anelastic model at annual period (middle). Differences (x10) are in the lower panels. Left/right groups: weak/strong frequency dependence of *Q*.

References

[1] Anderson DL, Kanamori H, Hart RS, Liu H-P (1977). The Earth as a seismic absorption band. *Science*, **196**(4294), 1104–1106.
[2] Anderson DL, Minster JB (1979). The frequency dependence of *Q* in the Earth and implications for mantle rheology and the Chandler wobble. *Geophys. J. R. astr. Soc.*, **58**, 431–440.
[3] Zschau J (1983). Rheology of the Earth's mantle at tidal and Chandler wobble periods. *Proc. 9th Intl. Symposium on Earth Tides*, 605–630.
[4] Benjamin D, Wahr J, Ray RD, Egbert GD, Desai SD (2006). Constraints on mantle anelasticity from geodetic observations, and implications for the J_2 anomaly. *Geophys. J. Int.*, **165**(1), 3–16.
[5] Dziewonski AM, Anderson DL (1981). Preliminary reference Earth model. *Phys. Earth Planet. Inter.* **25**, 297–356.
[5] Penna NT, Clarke PJ, Bos MS, Baker TF (2015). Ocean tide loading displacements in western Europe: 1. Validation of kinematic GPS estimates, *J. Geophys. Res*, **120**, 6523–6539.
[6] Bos MS, Penna NT, Baker TF, Clarke PJ (2015). Ocean tide loading displacements in western Europe: 2. GPS-observed anelastic dispersion in the asthenosphere, *J. Geophys. Res*, **120**, 6540–6557.
[7] Kustowski B, Ekström G, Dziewonski AM (2008). Anisotropic shear-wave velocity structure of the Earth's mantle: A global model, *J. Geophys. Res*, **113**, B06306.

Acknowledgements

Parts of this work were funded in the UK by NERC grants NE/C003438/1 and NE/J005789/1FCT and at UBI within project IDL-FCT-UID/GEO/50019/2013 and by grant SFRH/BPD/89923/2012. It would be impossible without continued free data and products from the International GNSS Service, the NERC BIGF, the IGN and EUREF.